PHYSICAL REVIEW FLUIDS **2**, 062801(R) (2017)

Turbulent heat transport regimes in a channel

B. Castaing*
Univ. Grenoble Alpes, CNRS, Grenoble INP, LEGI, F-38000 Grenoble, France

E. Rusaouën, J. Salort, and F. Chillà†
Univ Lyon, Ens de Lyon, Univ Claude Bernard, CNRS, Laboratoire de Physique, F-69342 Lyon, France
(Received 4 November 2016; published 14 June 2017)

In this paper we focus on the turbulent transport of a scalar through a channel. The scalar flux and the corresponding scalar concentration gradient along the channel allow us to define a Nusselt number and a Grashof number. While the relation between the large-scale velocity field and the input energy rate show perfect inertial (turbulent) behavior, three different regimes can be distinguished, with different scalings between Nusselt and Grashof numbers.

DOI: 10.1103/PhysRevFluids.2.062801

I. INTRODUCTION

In the past decade, scalar free convection in a tiltable channel appeared as an interesting model flow for evidencing the base mechanisms of convection [1–11]. Different regimes have been evidenced depending on the angle ψ between the channel axis and the vertical one, the Prandtl (or Schmidt) number ν/κ, or the amplitude of density differences. Here ν is the kinematic viscosity of the fluid and κ the diffusion coefficient of the active scalar.

The typical geometry is schematized in Fig. 1. A channel connects two chambers. The chambers have different temperatures in the case of heat transport and different scalar concentrations in the other cases. For the sake of clarity, we will concentrate on heat transport, speaking of temperature instead of scalar concentration and heat flux instead of scalar flux, but all what follows can be easily translated into the other language.

The Boussinesq equations are written

$$\partial_t v_i + v_j \partial_j v_i = -\frac{\partial_i p}{\rho} - g_i \alpha \vartheta + \nu \partial_j \partial_j v_i, \tag{1}$$

$$\partial_t \vartheta + v_j \partial_j \vartheta = \kappa \partial_j \partial_j \vartheta, \tag{2}$$

$$\partial_j v_j = 0, \tag{3}$$

where g is the gravitation acceleration, p the pressure, and ρ the density of the fluid. Within this Boussinesq approximation [12], the equations are the same, whether ϑ is the temperature (thermal case) or the solute concentration (scalar case). The last case generally allows us to work with large Prandtl (indeed Schmidt) numbers Pr, but caution must be taken to avoid mixed temperature and concentration effects (the Soret effect). Apart from these effects, a difference between these two cases can only come from non-Boussinesq effects, supposedly avoided in the experiments of interest here. The origin of ϑ is such that its mean value on the channel is zero. Also, α is the coefficient of thermal expansion.

*bernard.castaing627@laposte.net
†Francesca.Chilla@ens-lyon.fr

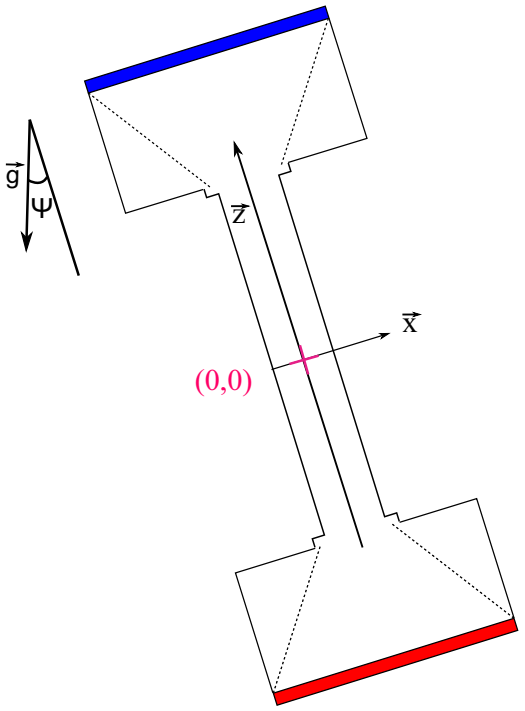

FIG. 1. Sketch of the typical cell showing the definition of the coordinates and of the inclination angle ψ.

The channel is sufficiently long to assume translational invariance along its axis (the z direction). Then the only characteristic length is d, the diameter of the channel for a circular one, its width for a square one. In these conditions, a uniform mean temperature (or scalar concentration) gradient develops along the channel:

$$\beta = -\frac{d\langle\vartheta\rangle}{dz}, \tag{4}$$

where $\langle\cdot\rangle$ stands for the local statistical average. The flow is governed by two nondimensional numbers, the Prandtl number Pr and the Grashof number

$$\mathrm{Gr} = \frac{g\alpha\beta d^4}{\nu^2}. \tag{5}$$

Sometimes, the Rayleigh number $\mathrm{Ra} = \mathrm{Gr}\,\mathrm{Pr}$ is used instead of Gr.

We are interested in the turbulent case, where the mean diffusive heat flux is negligible compared to the convective one. Multiplying Eq. (1) by v_i and averaging, in a globally stationary flow ($\partial_t\langle\cdot\rangle = 0$), it is easy to show that the kinetic energy input rate per unit mass ϵ is simply related to the heat flux Q_i [12],

$$\epsilon = -g_i\alpha\langle\vartheta v_i\rangle = -g_i\alpha\frac{Q_i}{C_p}, \tag{6}$$

where C_p is the heat capacity per unit volume; ϵ can also be expressed as

$$\epsilon = \nu\langle\partial_i v_j \partial_i v_j\rangle, \tag{7}$$

which gives a useful evaluation for the typical small-scale velocity gradients

$$\sqrt{\langle \partial_i v_j \partial_i v_j \rangle} = \left(\frac{\epsilon}{\nu}\right)^{1/2}. \tag{8}$$

A characteristic of the inertial regimes is that the large-scale velocity fluctuations, at constant inclination angle, scale as [6,7]

$$U_t = \left(\frac{Qdg\alpha}{C_p}\right)^{1/3}, \tag{9}$$

where d is the channel diameter and $Q = \overline{Q_z}$ is the average of Q_z on the cross section of the channel.

In the same regimes, in Eq. (1), inertial terms as $\partial_t v_i$, $v_j \partial_j v_i$, or $\partial_i p/\rho$ equilibrate with $g_i \alpha \vartheta$. This means that large-scale temperature fluctuations scale as $U_t^2/g\alpha d$. In spite of this great unity in the scaling behavior, three different regimes have been observed concerning the relation between the temperature (or scalar concentration) gradient β along the channel and the heat flux Q and thus between the Nusselt number

$$\mathrm{Nu} = \frac{Q}{C_p \kappa \beta} \tag{10}$$

and the Grashof number Gr.

Note that, in all the experiments, the flux Q is imposed and the gradient β measured. However, in numerical simulations [9,10], β is imposed and the flux Q is measured. At large Grashof number, every one [5,7,10,11] agrees with

$$\frac{\mathrm{Nu}}{\mathrm{Pr}} \propto \mathrm{Gr}^{1/2} \tag{11}$$

[sometimes expressed as $\mathrm{Nu} \propto (\mathrm{RaPr})^{1/2}$]. At lower Grashof number, Riedinger *et al.* [8] evidenced a regime

$$\mathrm{Nu} \propto \mathrm{Gr}^2 \tag{12}$$

without precision on the Prandtl number (Pr) dependence. Recently, Pawar and Arakeri [13] observed a regime

$$\frac{\mathrm{Nu}}{\mathrm{Pr}} \propto \mathrm{Gr}^{0.3}. \tag{13}$$

The purpose of this paper is to explain these regimes and to precisely determine their Pr dependence. We will show that the $\mathrm{Gr}^{0.3}$ regime can be intermediate between the two other ones and disappears for $\mathrm{Pr} < 1$. We call this regime the Batchelor regime (for reasons that appear below). In a similar way, the soft-turbulence regime (Gr^2) should disappear for $\mathrm{Pr} \gg 1$. Following Riedinger *et al.* [8], we call the $\mathrm{Nu} \propto \mathrm{Gr}^{1/2}$ regime the hard-turbulence [14] regime. We develop our arguments in the following section.

II. EVALUATION OF β

In this section we consider the flow as anisotropic, with a hot side going up and a cold side going down and stationary nonzero x profiles of the mean temperature and the mean axial (z) component of the velocity, as it is when the inclination angle ψ is sufficiently large. We explicitly consider the vertical case as the limit of the inclined case when ψ goes to zero. We are conscious that, in the vertical case, the flow is helicoidal, with a zero mean velocity [11], but we consider it as a slow precession of the anisotropic flow around the z axis [6].

Our evaluation of β will be based on two different expressions for the entropy production per unit volume $\dot{S}$. On the one hand, this entropy production can be related to the microscopic dissipative

temperature gradients

$$\dot{S} = C_p \kappa \frac{\langle \partial_i \vartheta \partial_i \vartheta \rangle}{T^2}, \tag{14}$$

where the absolute temperature $T = T_0 + \langle \vartheta \rangle$ and T_0 is the mean temperature of the channel. On the other hand, from a macroscopic point of view,

$$\dot{S} = -\frac{Q_i \partial_i T}{T^2}. \tag{15}$$

The temperature T can be written as

$$T = T_0 - \beta z + \Theta(x), \tag{16}$$

where $\Theta(x)$ is the transverse (x) profile of temperature. The scalar product of the heat flux and the mean temperature gradient is written

$$Q_i \partial_i T = Q_x \frac{d\Theta}{dx} - \beta Q_z. \tag{17}$$

Due to the conservation of energy, the transverse flux Q_x is related to the mean z velocity profile $U_z(x)$ through [8]

$$\frac{dQ_x}{dx} = C_p \beta U_z. \tag{18}$$

Thus, in all the inertial ranges, Q_x scales as $C_p \beta U_t d$. As for Θ, Eq. (1) implies that it scales as $U_t^2/g\alpha d$. In the end, using the definition of U_t, Eq. (9), $Q_x \frac{d\Theta}{dx}$, scales as

$$\frac{C_p \beta U_t^3}{g\alpha d} = \beta Q. \tag{19}$$

Comparing Eqs. (14), (15), and (17) gives a formal expression for β,

$$\beta = K_1 C_p \kappa \frac{\langle \partial_i \vartheta \partial_i \vartheta \rangle}{Q}, \tag{20}$$

where K_1 is a constant whose value is the same in all the inertial regimes, whether Batchelor, soft, or hard turbulence, but which can depend on the inclination angle ψ.

Calling $\theta = \vartheta - \langle \vartheta \rangle$ the temperature fluctuation and neglecting the average gradients compared to the instantaneous ones, $\langle \partial_i \vartheta \partial_i \vartheta \rangle$ can be evaluated as the mean-square fluctuation at the temperature dissipative scale $\langle \theta^2 \rangle_D$, divided by this dissipative scale η_θ squared:

$$\langle \partial_i \theta \partial_i \theta \rangle \simeq \frac{\langle \theta^2 \rangle_D}{\eta_\theta^2}. \tag{21}$$

The evaluation of $\langle \theta^2 \rangle_D$ and η_θ will differ, depending if the Prandtl number is larger or smaller than 1.

A. Small Prandtl number

Let us first assume that the Reynolds number is sufficient to have a Kolmogorov velocity inertial range, between the velocity correlation scale ℓ and the velocity dissipation scale η. At small Prandtl number, the temperature dissipative scale is larger than the velocity one: $\eta_\theta > \eta$. Here η_θ is such that the typical stirring frequency at this scale equals the dissipation frequency

$$\frac{v(\eta_\theta)}{\eta_\theta} \simeq \frac{U_t(\eta_\theta/\ell)^{1/3}}{\eta_\theta} \simeq \frac{\kappa}{\eta_\theta^2}, \tag{22}$$

where we assimilate the typical large-scale velocity with U_t, for the sake of simplicity in this order of magnitude evaluation. Clearly, this hides a constant that depends on the inclination angle ψ.

This qualitatively means that, at scales lower than η_θ, due to the rapidity of diffusion, stirring is unable to enhance the temperature gradients. The temperature dissipative scale η_θ can then be expressed as

$$\eta_\theta \simeq \ell \left(\frac{\kappa}{U_t \ell} \right)^{3/4}. \tag{23}$$

In Kolmogorov's approach, the temperature fluctuation at the scale η_θ is written [17]

$$\langle \theta^2 \rangle_D \simeq \langle \theta^2 \rangle \left(\frac{\eta_\theta}{\ell} \right)^{2/3}. \tag{24}$$

According to Eq. (1) and the resulting equilibrium between the buoyancy term $g_i \alpha \vartheta$ and the inertial terms [see the discussion after Eq. (9)], the mean-square temperature fluctuation $\langle \theta^2 \rangle$ in an inertial regime can be written

$$\langle \theta^2 \rangle = K_2 \frac{U_t^4}{(g\alpha\ell)^2}, \tag{25}$$

where again K_2 is a constant whose value is the same in all the inertial regimes, but which can depend on the inclination angle ψ. Using Eqs. (21) and (23)–(25), we have thus the estimate for $\langle \partial_i \theta \partial_i \theta \rangle$,

$$\langle \partial_i \theta \partial_i \theta \rangle \simeq K_2 \frac{U_t^4}{(g\alpha\ell)^2} \left(\frac{\eta_\theta}{\ell} \right)^{2/3} \frac{1}{\eta_\theta^2} = K_2 \frac{U_t^4}{(g\alpha\ell^2)^2} \left(\frac{\eta_\theta}{\ell} \right)^{-4/3} \tag{26}$$

$$= K_2 \frac{U_t^4}{(g\alpha\ell^2)^2} \frac{U_t \ell}{\kappa} = K_2 \frac{U_t^5}{\kappa (g\alpha)^2 \ell^3}, \tag{27}$$

and for β, using Eqs. (9) and (20),

$$\beta \simeq K_1 K_2 \frac{\kappa d g \alpha}{U_t^3} \frac{U_t^5}{\kappa (g\alpha)^2 \ell^3} = K_1 K_2 \frac{U_t^2 d}{g\alpha\ell^3}. \tag{28}$$

Combining Eqs. (28) and (9), the Nusselt number Nu is given by

$$\frac{\mathrm{Nu}}{\mathrm{Pr}} = \frac{Q}{C_p \nu \beta} = \frac{U_t^3}{d g \alpha \nu \beta}. \tag{29}$$

We now can write, using Eq. (28),

$$\frac{\mathrm{Nu}}{\mathrm{Pr}} \simeq \left(\frac{\beta g \alpha \ell^3}{K_1 K_2 d} \right)^{3/2} \frac{1}{d g \alpha \nu \beta} = \left(\frac{1}{K_1 K_2} \right)^{3/2} \left(\frac{\ell}{d} \right)^{9/2} \left(\frac{g \alpha \beta d^4}{\nu^2} \right)^{1/2} = A\, \mathrm{Gr}^{1/2}, \tag{30}$$

where A is a constant that can depend on the inclination angle ψ. We thus find, as expected, the hard-turbulence (HT) regime.

At lower Reynolds numbers, the temperature dissipative scale η_θ joins ℓ [17]. We simply have to make $\eta_\theta = \ell$ in Eq. (26):

$$\langle \partial_i \theta \partial_i \theta \rangle \simeq K_2 \frac{U_t^4}{(g\alpha\ell^2)^2}. \tag{31}$$

Then

$$\beta \simeq K_1 K_2 \frac{\kappa d g \alpha}{U_t^3} \frac{U_t^4}{(g\alpha\ell^2)^2} = K_1 K_2 \frac{\kappa U_t d}{g\alpha\ell^4} \tag{32}$$

and

$$\frac{\mathrm{Nu}}{\mathrm{Pr}} \simeq \left(\frac{\beta g \alpha \ell^4}{K_1 K_2 d\kappa}\right)^3 \frac{1}{dg\alpha\nu\beta} = \left(\frac{1}{K_1 K_2}\right)^3 \left(\frac{\ell}{d}\right)^{12} \left(\frac{g\alpha\beta d^4}{\nu^2}\right)^2 \left(\frac{\nu}{\kappa}\right)^3 = B\,\mathrm{Pr}^3\mathrm{Gr}^2, \tag{33}$$

where B is a constant that can depend on the inclination angle ψ. This is the soft-turbulence (ST) scaling. It coincides with the absence of inertial range for the scalar, but not for the velocity: as $\eta_\theta > \eta$, we yet have $\ell > \eta$. The two scalings above can be presented as

$$\mathrm{Nu} = A(\mathrm{Gr}\,\mathrm{Pr}^2)^{1/2}, \quad \mathrm{Nu} = B(\mathrm{Gr}\,\mathrm{Pr}^2)^2, \tag{34}$$

which shows that in a diagram of Nu versus $\mathrm{Gr}\,\mathrm{Pr}^2$ all the data corresponding to different (small) Prandtl numbers should merge on a single curve (at constant inclination angle ψ).

B. High Prandtl number

When the Prandtl number is large, the high-Reynolds-number situation is different. Indeed, the Kolmogorov inertial range is followed by a Batchelor range of scales [20] in which the temperature fluctuations remain approximately constant. The temperature dissipative scale η_θ is now smaller than the velocity one η:

$$\frac{v(\eta_\theta)}{\eta_\theta} = \frac{v(\eta)}{\eta} \simeq \left(\frac{\epsilon}{\nu}\right)^{1/2} = \left(\frac{U_t^3}{d\nu}\right)^{1/2} \simeq \frac{\kappa}{\eta_\theta^2}. \tag{35}$$

On the other hand,

$$\langle\theta^2\rangle_D \simeq \langle\theta^2\rangle \left(\frac{\eta}{\ell}\right)^{2/3} \simeq K_2 \frac{U_t^4}{(g\alpha\ell)^2} \left(\frac{\nu^3 d}{U_t^3 \ell^4}\right)^{1/6}. \tag{36}$$

Using Eqs. (20), (21), (35), and (36), we have

$$\beta \simeq K_1 K_2 \frac{g\alpha d}{U_t^3} \left(\frac{U_t^3}{d\nu}\right)^{1/2} \frac{U_t^{7/2} \nu^{1/2} d^{1/6}}{(g\alpha\ell)^2 \ell^{2/3}} = K_1 K_2 \frac{U_t^2}{g\alpha d^2} \left(\frac{d}{\ell}\right)^{8/3} \tag{37}$$

and using Eq. (29),

$$\frac{\mathrm{Nu}}{\mathrm{Pr}} = \frac{U_t^3}{dg\alpha\nu\beta} \simeq \frac{1}{dg\alpha\nu\beta} \left(\frac{g\alpha\beta d^2}{K_1 K_2}\right)^{3/2} \left(\frac{\ell}{d}\right)^4 = C\,\mathrm{Gr}^{1/2}, \tag{38}$$

where C is fixed at constant inclination angle ψ. This is the HT regime.

At lower Reynolds number, η reaches ℓ, there is no Kolmogorov inertial range, but the velocity gradients continue to smooth down, and the temperature dissipative scale η_θ continues its growth as [see Eq. (35)]

$$\frac{\kappa}{\eta_\theta^2} \simeq \left(\frac{U_t^3}{d\nu}\right)^{1/2}. \tag{39}$$

In the absence of inertial range, $\langle\theta^2\rangle_D \simeq \langle\theta^2\rangle$ and, using Eqs. (20) and (21),

$$\beta \simeq K_1 K_2 \frac{g\alpha d}{U_t^3} \frac{U_t^4}{(g\alpha\ell)^2} \left(\frac{U_t^3}{d\nu}\right)^{1/2} = K_1 K_2 \frac{U_t^{5/2}}{g\alpha\nu^{1/2} d^{3/2}} \left(\frac{d}{\ell}\right)^2. \tag{40}$$

As in the previous cases, we can extract the expression of U_t versus β,

$$U_t \simeq \left(\frac{g\alpha\beta\nu^{1/2} d^{3/2}}{K_1 K_2}\right)^{2/5} \left(\frac{\ell}{d}\right)^{4/5}, \tag{41}$$

and use it in the expression of Nu/Pr,

$$\frac{\mathrm{Nu}}{\mathrm{Pr}} = \frac{U_t^3}{dg\alpha\nu\beta} \simeq \left(\frac{1}{K_1K_2}\right)^{6/5}\left(\frac{g\alpha\beta d^4}{\nu^2}\right)^{1/5}\left(\frac{\ell}{d}\right)^{12/5} = E\,\mathrm{Gr}^{1/5}, \tag{42}$$

where E is fixed at constant inclination angle ψ. While the resulting exponent (0.2) differs from the Pawar *et al.* [13] one (0.3), these regimes nicely correspond in other aspects. Indeed, plotting Nu/Pr versus Gr, all Prandtl number merge on a single curve, as observed by Pawar *et al.* Moreover, as this regime occurs between $\mathrm{Gr}^{1/2}$ and Gr^2 (see below) regimes, it appears as an inflection point whose slope hardly reaches the asymptotic one. We call this regime the Batchelor regime. Finally, if the Prandtl number is not too high in such a way that η_θ reaches ℓ [17] while the flow is always in a turbulent inertial regime, η_θ cannot grow further. Then

$$\langle \partial_i\theta\partial_i\theta\rangle \simeq \frac{\langle\theta^2\rangle}{\ell^2} \tag{43}$$

and, using Eqs. (9), (20), and (25),

$$\beta \simeq K_1K_2\frac{g\alpha d}{U_t^3}\frac{U_t^4}{(g\alpha\ell)^2}\frac{\kappa}{\ell^2} = K_1K_2\frac{U_t\kappa}{g\alpha d^4}\left(\frac{d}{\ell}\right)^4. \tag{44}$$

Then, using Eq. (29),

$$\frac{\mathrm{Nu}}{\mathrm{Pr}} = \frac{U_t^3}{dg\alpha\nu\beta} \simeq \left(\frac{1}{K_1K_2}\right)^{3}\left(\frac{g\alpha\beta d^4}{\kappa^2}\right)^{2}\frac{\kappa}{\nu}\left(\frac{\ell}{d}\right)^{12} = B'\mathrm{Gr}^2\mathrm{Pr}^3, \tag{45}$$

where B' is a constant at constant inclination angle ψ. This is the moderate Prandtl soft-turbulence scaling, which can also be written $\mathrm{Nu} = B'(\mathrm{Gr}\,\mathrm{Pr}^2)^2$, and it is identical to the small Prandtl soft turbulence ($B' = B$).

III. DISCUSSION AND CONCLUSION

Let us thus sum up the succession of inertial regimes, starting from the highest Grashof numbers and going down. When the Prandtl number is low, the HT regime corresponds to the relation

$$\mathrm{Nu} = A(\mathrm{Gr}\,\mathrm{Pr}^2)^{1/2}. \tag{46}$$

At lower Grashof number, but sufficient to have an inertial regime, we should have the ST regime, where

$$\mathrm{Nu} = B(\mathrm{Gr}\,\mathrm{Pr}^2)^2. \tag{47}$$

The transition corresponds to the *temperature* dissipative scale reaching the large correlation scale [17]. On a Nu versus $\mathrm{Gr}\,\mathrm{Pr}^2$ diagram, all the (small) Prandtl numbers should merge on the same curve. When the Prandtl number is large, which is typically the case for dilute solutions of salt, the highest Grashof numbers again correspond to the HT regime

$$\frac{\mathrm{Nu}}{\mathrm{Pr}} = C\,\mathrm{Gr}^{1/2}. \tag{48}$$

At lower Grashof number, but sufficient to have an inertial regime, we should have the Batchelor regime

$$\frac{\mathrm{Nu}}{\mathrm{Pr}} = E\,\mathrm{Gr}^{1/5}. \tag{49}$$

The transition corresponds to the *velocity* dissipative scale reaching the large correlation scale, thus to the Kolmogorov inertial range vanishing. On a Nu/Pr versus Gr diagram, all the (high) Prandtl numbers merge on the same curve. At even lower Grashof number, but always sufficient to have an

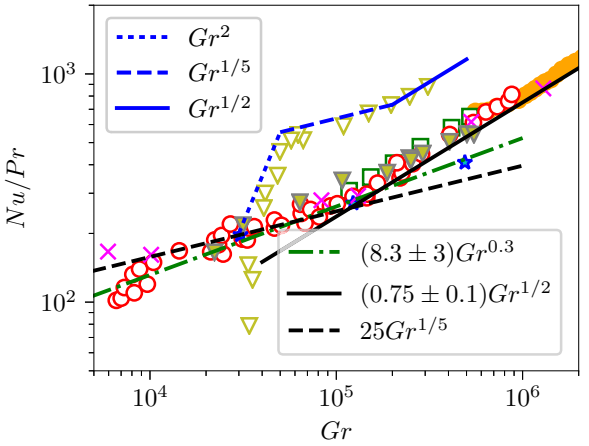

FIG. 2. Open and closed circles, squares, stars, and crosses are data extracted from Pawar and Arakeri's article [13]. Brine experiment results, with Pr $\simeq$ 600, are shown as closed orange circles [13], open green squares [11], and magenta crosses [21]. They correspond to our high Prandtl numbers. Heat experiment results, with Pr $\simeq$ 6, are shown as open red circles [13] and closed triangles [22] and open triangles [8]. They correspond to our moderate Prandtl numbers. Note that the latter are for $\psi = 5^\circ$ while all the other data shown are for the vertical case. Numerical study results, with Pr = 1, are shown as blue stars. They correspond to the limit between small and moderate Prandtl numbers. The data of [22], once their Grashof number is multiplied by $16/\pi^2$, show good agreement with that of Pawar and Arakeri [13], despite the difference in the cross sections. Solid lines correspond to hard turbulence, dashed lines correspond to the Batchelor regime, and the blue dotted line corresponds to the soft turbulence (for the 5° case, from Ref. [8]). The green dash-dotted line shows Pawar and Arakeri's interpretation, which fits the data as well, but could be influenced by the lowest Gr data that could correspond to the transition toward soft turbulence (with moderate Prandtl number; see Fig. 3).

inertial regime (thus for moderate Prandtl numbers), we should find again the ST regime, Eq. (47). Again, the transition corresponds to the temperature dissipative scale reaching the large correlation scale [17].

In Fig. 2 we represent various data, extracted from Refs. [8,13,22], on a log-log plot of Nu/Pr versus Gr. The data of Ref. [13] all correspond to a circular channel, the characteristic length d being the diameter. The data of Refs. [8,22] correspond to a square channel, d being one side of the square. Thus, we multiplied this last d by $\sqrt{4/\pi}$ in such a way that $\pi d^2/4$ always represents the cross section of the channel. It is equivalent to multiplying their Grashof numbers by $16/\pi^2$. The agreement between the series of data of Refs, [13] (open circles) and [22] (closed triangles) is then good. These data should correspond to moderate Prandtl numbers, obtained with water, the scalar being the temperature.

Closed circles [13], open squares [11], and crosses [21] correspond to brine experiments, with a large Prandtl number (Pr = 600). As remarked in Ref. [13], they nicely merge with the previous ones in this diagram, both in the high-Gr HT regime (Nu/Pr $\propto$ $\mathrm{Gr}^{1/2}$) and in the lower Gr one. The latter fits as well with the predicted $\mathrm{Gr}^{0.2}$ (Batchelor regime) as with the $\mathrm{Gr}^{0.3}$ proposed by [13]. However, the lower Grashof open circle data, which influence the $\mathrm{Gr}^{0.3}$ choice, could correspond to a transition toward the soft turbulence, which is better visible with the $\psi = 5^\circ$ data (open triangles [8]).

Unfortunately, we have no experimental data really corresponding to small Prandtl values. The numerical simulation [10] (stars in Fig. 2), which correspond to Pr = 1, has larger error bars than the experiments and should anyway lay at the frontier between small and moderate Prandtl numbers. This range should be carefully examined in future studies.

All these data help to propose a map of the different regimes, at least for the vertical case (see Fig. 3). The transition toward the laminar regime at the lowest Gr is assumed to correspond to a

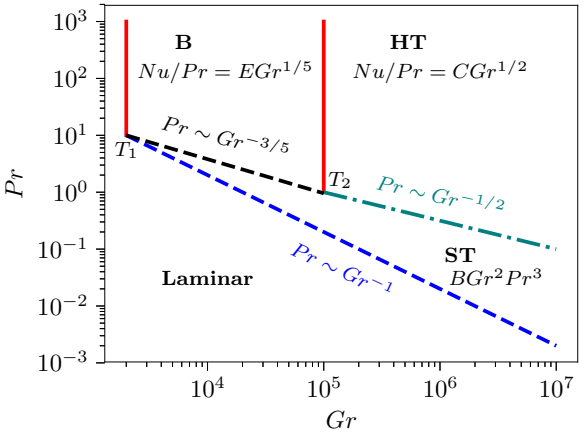

FIG. 3. Schematic diagram showing the various regimes in the plane (Gr,Pr) on a logarithmic scale. The diagram corresponds to the vertical case, which allows considering that the laminar to turbulent transition occurs at the same Reynolds number Re, whatever Pr. Considering that $\mathrm{Re} \simeq U_t d/\nu = (\mathrm{NuGr/Pr})^{1/3}$ in all the inertial regimes, we obtain Gr = const for the laminar-Batchelor (B) transition and GrPr = const for the laminar–soft-turbulence transition. For the other transitions, we identify the two expressions of Nu on both sides, which gives Gr = const for the Batchelor–hard turbulence transition, GrPr^2 = const for the soft-turbulence–hard-turbulence one, and $\mathrm{GrPr}^{5/3}$ = const for the soft-turbulence–Batchelor one. The existence of the moderate Prandtl number range, where the soft-turbulence, Batchelor, and hard-turbulence regimes follow one another when raising Gr at constant Pr, is clear from this diagram. The exact positions of the two triple points T1 and T2 need to be experimentally determined precisely, but an order of magnitude estimation could be Pr = 10 and $\mathrm{Gr} = 2\times10^3$ for T1 and Pr = 1 and $\mathrm{Gr} = 10^5$ for T2.

fixed Reynolds number. In the adjacent inertial regime, the Reynolds number always correspond to

$$\mathrm{Re} \propto \frac{U_t d}{\nu} = (\mathrm{Nu\,Gr/Pr})^{1/3}. \tag{50}$$

All the other frontiers are determined by the continuity of Nu. They merge at two triple points, which we tentatively place at T_1 (Pr = 10 and $\mathrm{Gr} = 2\times10^3$) and T_2 (Pr = 1 and $\mathrm{Gr} = 10^5$). The moderate Prandtl numbers correspond to the range between T_1 and T_2, $1 \lesssim \mathrm{Pr} \lesssim 10$.

We find thus all the observed regimes [8,13] if we identify the predicted exponent for the Batchelor regime (0.2) to the observed one [13] (0.3). Moreover, these regimes nicely underline the existence of the Kolmogorov or Batchelor ranges of scales and their clear-cut transitions.

ACKNOWLEDGMENT

We thank the referees for several interesting propositions and comments.

[1] T. Seon, J. P. Hulin, D. Salin, B. Perrin, and E. J. Hinch, Laser-induced fluorescence measurements of buoyancy driven mixing in tilted tubes, Phys. Fluids **18**, 041701 (2006).

[2] J. Znaien, Y. Hallez, F. Moisy, J. Magnaudet, J. P. Hulin, D. Salin, and E. J. Hinch, Experimental and numerical investigations of flow structure and momentum transport in a turbulent buoyancy-driven flow inside a tilted tube, Phys. Fluids **21**, 115102 (2009).

[3] J. Znaien, F. Moisy, and J. P. Hulin, Flow structure and momentum transport for buoyancy driven mixing flows in long tubes at different tilt angles, Phys. Fluids **23**, 035105 (2011).

[4] R. Delgado-Buscalioni and E. Crespo, Flow and heat transfer regimes in inclined differentially heated cavity, Int. J. Heat Mass Transfer **44**, 1947 (2001).
[5] M. Gibert, H. Pabiou, F. Chillà, and B. Castaing, High-Rayleigh-Number Convection in a Vertical Channel, Phys. Rev. Lett. **96**, 084501 (2006).
[6] M. Gibert, H. Pabiou, J.-C. Tisserand, B. Gertjerenken, B. Castaing, and F. Chillà, Heat convection in a vertical channel: Plumes versus turbulent diffusion, Phys. Fluids **21**, 035109 (2009).
[7] J.-C. Tisserand, M. Creyssels, M. Gibert, B. Castaing, and F. Chillà, Convection in a vertical channel, New J. Phys. **12**, 075024 (2010).
[8] X. Riedinger, J.-C. Tisserand, F. Seychelles, B. Castaing, and F. Chillà, Heat transport regimes in an inclined channel, Phys. Fluids **25**, 015117 (2013).
[9] E. Calzavarini, D. Lohse, F. Toschi, and R. Tripiccione, Rayleigh and Prandtl number scaling in the bulk of Rayleigh-Bénard turbulence, Phys. Fluids **17**, 055107 (2005).
[10] L.-E. Schmidt, E. Calzavarini, D. Lohse, F. Toschi, and R. Verzicco, Axially homogeneous Rayleigh-Bénard convection in a cylindrical cell, J. Fluid Mech. **691**, 52 (2012).
[11] M. R. Cholemari and J. H. Arakeri, Axially homogeneous, zero mean flow buoyancy-driven turbulence in a vertical pipe, J. Fluid Mech. **621**, 69 (2009).
[12] D. J. Tritton, *Physical Fluid Dynamics* (Oxford University Press, Oxford, 1988), Chaps. 13 and 14.
[13] S. S. Pawar and J. H. Arakeri, Two regimes of flux scaling in axially homogeneous turbulent convection in vertical tube, Phys. Rev. Fluids **1**, 042401(R) (2016).
[14] The term "hard turbulence" (as well as "soft turbulence") was coined by Heslot *et al.* [15], in the context of Rayleigh-Bénard convection. The transition from soft to hard was associated with the apparition of a scaling range in temperature spectra, together with a change in the temperature histograms shape, without a clear relation between these two characteristics. In his review, Siggia [16] reproaches this lack of precision. Here the apparition of an inertial range when one enters the hard-turbulence regime justifies this appellation by Riedinger *et al.*
[15] F. Heslot, B. Castaing, and A. Libchaber, Transitions to turbulence in helium gas, Phys. Rev. A **36**, 5870 (1987).
[16] E. D. Siggia, High Rayleigh number convection, Annu. Rev. Fluid Mech. **26**, 137 (1994).
[17] One may wonder why we do not consider the possibility of a Bolgiano range where $\langle\theta^2\rangle_r$ depends on the scale r as $r^{2/5}$, down to a Bolgiano scale ℓ_B. Such a range has often been reported in convection flows [18,19]. However, the corresponding velocity structure function behavior (scaling as $r^{6/5}$) has never been observed. Moreover, ℓ_B should be of order ℓ and it is never envisaged that η_θ is larger than ℓ_B. Thus, the limit of the soft turbulence could simply correspond to $\eta_\theta = \ell_B$ rather than ℓ, without any change in the conclusions.
[18] F. Chillà, S. Ciliberto, C. Innocenti, and E. Pampaloni, Spectra of local and averaged scalar fields in turbulence, Europhys. Lett. **22**, 23 (1993).
[19] S. S. Pawar and J. H. Arakeri, Kinetic energy and scalar spectra in high Rayleigh number axially homogeneous buoyancy driven turbulence, Phys. Fluids **28**, 065103 (2016).
[20] H. Tennekes and J. Lumley, *A First Course in Turbulence* (MIT Press, Cambridge, 1972).
[21] R. O. Tovar, Ph.D. thesis, Universidad Nacional Autonoma de Mexico (2002).
[22] E. Rusaouën, Échanges turbulents en convection thermique, Ph.D. thesis, ENS de Lyon (2014).